Supplementary Information

Reversible-jump MCMC reveals binary black hole subpopulations with distinct redshift evolution

1 Population-weighted posteriors and probabilities

In this section, we analyze the population-weighted posteriors of individual events as well as their posterior probabilities of subpopulation membership, in light of the astrophysical interpretations in the main text.

Formalism. In order to examine the posterior probability that each individual observed event belongs in each subpopulation, we derive expressions for the posterior probability of the source parameters $\boldsymbol{\theta}_i$ of event i given the data $\{d\}$.

Let $k = 1, 2, \ldots, n$ index the subpopulations of a given model (of fixed dimensionality), and k_i denote the membership of event i to subpopulation k. From Bayes' theorem, the probability that event i belongs to subpopulation k conditioned on the data and population parameters $\{\boldsymbol{\lambda}\}, \boldsymbol{\Lambda}$ is given by

$$p(k_i|\{d\}) \propto \int \mathrm{d}\{\boldsymbol{\lambda}\}\mathrm{d}\boldsymbol{\Lambda}\, \mathcal{L}(d_i|k_i, \{\boldsymbol{\lambda}\}, \boldsymbol{\Lambda})\, p(k_i|\{\boldsymbol{\lambda}\}, \boldsymbol{\Lambda})\, p(\{\boldsymbol{\lambda}\}, \boldsymbol{\Lambda}|\{d\}_{\neq i}). \tag{1}$$

$p(\{\boldsymbol{\lambda}\}, \boldsymbol{\Lambda}|\{d\}_{\neq i})$ is the "leave-one-out" posterior probability of the hyperparameters that condition on the data of all events except for event i, to avoid double counting. This is related to the posterior probability of the full analysis via

$$p(\{\boldsymbol{\lambda}\}, \boldsymbol{\Lambda}|\{d\}_{\neq i}) \propto \frac{p(\{\boldsymbol{\lambda}\}, \boldsymbol{\Lambda}|\{d\})}{\mathcal{L}(d_i|\{\boldsymbol{\lambda}\}, \boldsymbol{\Lambda})} \tag{2}$$

taking advantage of the fact that the event-level likelihoods factorize. In Eq. (1), $p(k_i|\{\boldsymbol{\lambda}\}, \boldsymbol{\Lambda})$ is the probability of event i belonging to subpopulation k_i given the population; it has no dependence on $\{d\}_{\neq i}$ since it is conditionally independent of the other events' data given the population parameters. It is given by

$$p(k_i|\{\boldsymbol{\lambda}\}, \boldsymbol{\Lambda}) = \frac{N_{k_i}(\boldsymbol{\lambda}_{k_i}, \boldsymbol{\Lambda})}{N(\{\boldsymbol{\lambda}\}, \boldsymbol{\Lambda})} \tag{3}$$

where $N_k(\boldsymbol{\lambda}_k, \boldsymbol{\Lambda})$ is the total expected number of mergers of subpopulation k, obtained by integrating its differential merger rate over $\boldsymbol{\theta}$.

The likelihood of d_i given that it belongs to subpopulation k_i and population parameters is

$$\mathcal{L}(d_i|k_i, \{\boldsymbol{\lambda}\}, \boldsymbol{\Lambda}) = \int \mathrm{d}\boldsymbol{\theta}\, \frac{\mathcal{L}(d_i|\boldsymbol{\theta})}{N_{k_i}(\boldsymbol{\lambda}_{k_i}, \boldsymbol{\Lambda})} \frac{\mathrm{d}N_{k_i}}{\mathrm{d}\boldsymbol{\theta}}(\boldsymbol{\lambda}_{k_i}, \boldsymbol{\Lambda}). \tag{4}$$

This can be approximated as a Monte Carlo sum over event i's posterior samples $\boldsymbol{\theta}_i^p$

$$\mathcal{L}(d_i|k_i, \{\boldsymbol{\lambda}\}, \boldsymbol{\Lambda}) \propto\approx \sum_p \frac{1}{\pi_{\mathrm{PE}}(\boldsymbol{\theta}_i^p)} \frac{1}{N_{k_i}(\boldsymbol{\lambda}_{k_i}, \boldsymbol{\Lambda})} \frac{\mathrm{d}N_{k_i}}{\mathrm{d}\boldsymbol{\theta}}(\boldsymbol{\lambda}_{k_i}, \boldsymbol{\Lambda}). \tag{5}$$

Eq. (1) can finally be computed by multiplying together Eqs. (2), (3) and (5) and expressing the integral as a sum over population posterior samples $\{\boldsymbol{\lambda}^m\}, \boldsymbol{\Lambda}^m$

$$p(k_i|\{d\}) \propto\approx \sum_p \frac{1}{\pi_{\mathrm{PE}}(\boldsymbol{\theta}_i^p)} \sum_m \frac{\mathrm{d}N_{k_i}}{\mathrm{d}\boldsymbol{\theta}}(\boldsymbol{\lambda}_{k_i}^m, \boldsymbol{\Lambda}^m)\Big|_{\boldsymbol{\theta}_i^p} \Big[N(\{\boldsymbol{\lambda}^m\}, \boldsymbol{\Lambda}^m)\, \mathcal{L}(d_i|\{\boldsymbol{\lambda}^m\}, \boldsymbol{\Lambda}^m)\Big]^{-1} \tag{6}$$

which is what we used to compute the probabilities shown below in Extended Data Fig. 2. The bracketed quantities can be pre-computed for each population posterior sample m; $\mathcal{L}(d_i|\{\boldsymbol{\lambda}^m\}, \boldsymbol{\Lambda}^m)$ can also be computed via Monte Carlo integration, marginalizing Eq. (4) over the different subpopulations

$$\mathcal{L}(d_i|\{\boldsymbol{\lambda}\}, \boldsymbol{\Lambda}) \propto\approx \sum_p \frac{1}{\pi_{\mathrm{PE}}(\boldsymbol{\theta}_i^p)} \frac{1}{N(\{\boldsymbol{\lambda}\}, \boldsymbol{\Lambda})} \sum_k \frac{\mathrm{d}N_k}{\mathrm{d}\boldsymbol{\theta}}(\boldsymbol{\lambda}_k, \boldsymbol{\Lambda}). \tag{7}$$

Next, the population-weighted posterior

$$p(\boldsymbol{\theta}_i|\{d\}) \propto \mathcal{L}(d_i|\boldsymbol{\theta}_i) p(\boldsymbol{\theta}_i|\{d\}_{\neq i}) \tag{8}$$

can be obtained in a similar manner, following ref. [1]:

$$p(\boldsymbol{\theta}_i|\{d\}) \propto\approx \frac{p(\boldsymbol{\theta}_i|d_i)}{\pi_{\mathrm{PE}}(\boldsymbol{\theta}_i)} \sum_k \sum_m \frac{\mathrm{d}N_k}{\mathrm{d}\boldsymbol{\theta}}(\boldsymbol{\lambda}_k^m, \boldsymbol{\Lambda}^m)\Big|_{\boldsymbol{\theta}_i} \Big[N(\{\boldsymbol{\lambda}^m\}, \boldsymbol{\Lambda}^m)\, \mathcal{L}(d_i|\{\boldsymbol{\lambda}^m\}, \boldsymbol{\Lambda}^m)\Big]^{-1}. \tag{9}$$

In practice, we assign each posterior sample $\boldsymbol{\theta}_i^p$ a weight

$$w_i^p \propto \frac{1}{\pi_{\mathrm{PE}}(\boldsymbol{\theta}_i^p)} \sum_k \sum_m \frac{\mathrm{d}N_k}{\mathrm{d}\boldsymbol{\theta}}(\boldsymbol{\lambda}_k, \boldsymbol{\Lambda})\Big|_{\boldsymbol{\theta}_i^p} \Big[N(\{\boldsymbol{\lambda}^m\}, \boldsymbol{\Lambda}^m)\, \mathcal{L}(d_i|\{\boldsymbol{\lambda}^m\}, \boldsymbol{\Lambda}^m)\Big]^{-1} \tag{10}$$

from which we can use a kernel density estimator to create the contours in Fig. 5 and Extended Data Fig. 1.

Individual events. Extended Data Fig. 1 shows the default `skewt` 3-component model's population-weighted posteriors of all analyzed events in m_1 and $\chi_{\rm eff}$. Events which are likely ($> 75\%$) to belong to one subpopulation are color-coded accordingly; otherwise, they are plotted in gray.

We identify these events in Extended Data Fig. 2, which shows the default model's subpopulation probabilities of the top 10 most confident events in each subpopulation, as well as the top 10 most ambiguous events. We then compare this to the subpopulation probabilities of the `NPLNP` 1 power-law + 2 Gaussians model of the same events, which we plot to the right. All events that are confidently detected in each subpopulation in the `skewt` population model are also confidently detected in the `NPLNP` model, supporting the robustness of these subpopulations.

The high-spin continuum subpopulation contains many of the exceptional events in the catalog in at least one of our population models. These include GW190412 [2], which is notable for its highly asymmetric masses, as well as GW231123 [3], which is both notable for their high masses and spins. GW190412 has also been identified as a candidate for an active galactic nucleus (AGN) disk-driven hierarchical merger origin [4–6], and both chemically homogeneous evolution (CHE) [7] and hierarchical AGN-disk mergers [8, 9] have been proposed as formation scenarios for GW231123. Additionally, the primary spin of GW190412 is too low [10] and the spins of GW231123 too high [11] for a cluster hierarchical merger scenario. Nonetheless the high-spin continuum subpopulation does contain most of the events identified as candidates for hierarchical mergers in previous works, including GW190517_055101, GW231028_153006 [12], GW231118_005626 [13], GW190519_153544, GW190620_030421, and GW190706_222641 [14]. This further emphasizes the ambiguous astrophysical interpretation of this subpopulation.

We can also examine the population-weighted posteriors of the O4b exceptional events GW241011 and GW241110 [15, 16], which we show in Extended Data Fig. 1. These events are identified as the most likely candidates for containing a black hole (BH) with a hierarchical origin [12, 13, 15], although we do not include them in our population analysis (as doing so would constitute essentially adding two events to the population by hand). With the `skewt` (`NPLNP`) population model, we find that the probability that GW241011 belongs in the high-spin continuum is 90.4% (99.9996%), while the corresponding probability for GW241110 is 35% (91%). This is consistent with the ambiguous astrophysical interpretation of this subpopulation, especially in the `skewt` population model. It is important to note that because both events have exceptional spins, including them in the population analysis has the potential to significantly change the properties of this subpopulation. Furthermore, because we only use $\chi_{\rm eff}$ rather than the full component spin vectors, we are not sensitive to more specific predictions of the hierarchical merger channel, such as the expectation for one or more of the component BHs to have spin magnitude $\chi \approx 0.7$ [17, 18]. Reapplying our framework to the full O4b catalog, and possibly expanding to more spin parameters, will constitute an important next step for finding a robust subpopulation of hierarchical mergers.

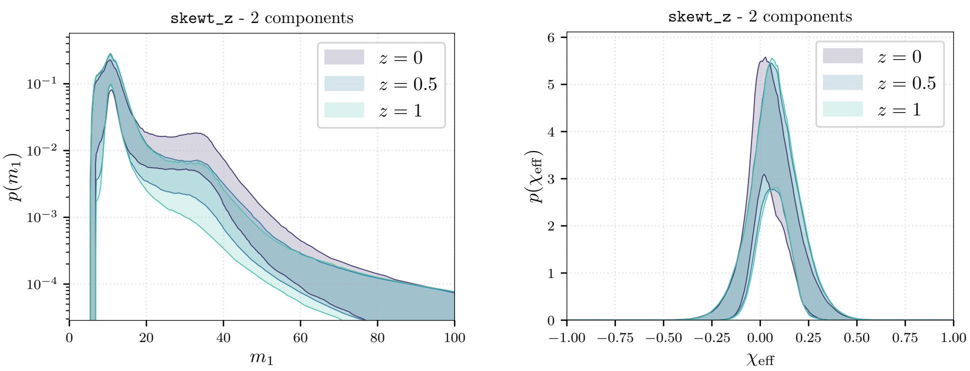

(a) (b)

Supplementary Fig. 1: 90% credibility intervals on the marginal distributions of (a) m_1 and (b) $\chi_{\rm eff}$ at $z = 0$, $z = 0.5$, and $z = 1$.

2 Correlations including spins

Previous works have found a broadening of the $\chi_{\rm eff}$ distribution with redshift [19, 20] and a correlation between mass ratio and $\chi_{\rm eff}$ [21–23], although evidence for the latter has become more ambiguous in the latest dataset [24]. We find no strong evidence for either of these correlations in our analysis, which we show in Fig. 1 and Supplementary Fig. 1. Our results suggest that the broadening of the $\chi_{\rm eff}$ distribution with redshift is either driven by an intrinsic evolution of the BH spin distribution, or by subpopulations with more complex redshift evolution than can be accommodated by a power law (e.g., subpopulations localized within a narrower range of redshifts). This stands in contrast with the results of ref. [20]; we note, however, that their analysis included the two remarkable O4b events GW241110 and GW241011, and employed a population model specifically designed to target a subpopulation of hierarchical mergers.

References

[1] Galaudage, S., Talbot, C., Thrane, E.: Gravitational-wave inference in the catalog era: Evolving priors and marginal events. Physical Review D **102**, 083026 (2020) https://doi.org/10.1103/PhysRevD.102.083026

[2] Abbott, R., Abbott, T.D., Abraham, S., Acernese, F., Ackley, K., *et al.*, : GW190412: Observation of a binary-black-hole coalescence with asymmetric masses. Physical Review D **102**, 043015 (2020) https://doi.org/10.1103/PhysRevD.102.043015

[3] Abac, A.G., Abouelfettouh, I., Acernese, F., Ackley, K., Adamcewicz, C., *et al.*, : GW231123: A Binary Black Hole Merger with Total Mass 190-265 M⊙. The Astrophysical Journal **993**, 25 (2025) https://doi.org/10.3847/2041-8213/ae0c9c

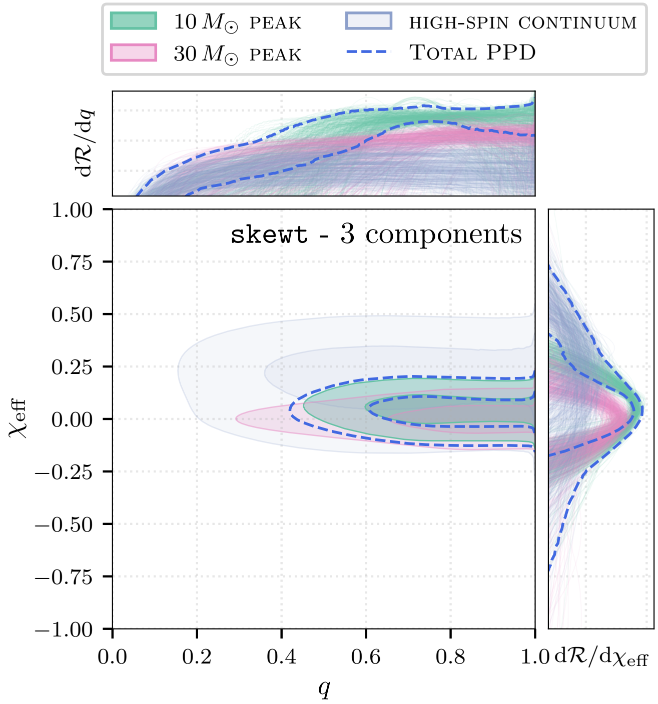

Fig. 1: 50% and 90% contours of the median posterior $\mathrm{d}\mathcal{R}^k/\mathrm{d}q\,\mathrm{d}\chi_{\mathrm{eff}}$ for each subpopulation k, evaluated at $z = 0.2$ in the `skewt` model; opacity of the shading corresponds to the relative rates of the subpopulations. Corresponding posterior sample draws of the marginalized 1D distributions (in log-scale) are shown in the side panels.

[4] Tagawa, H., Kocsis, B., Haiman, Z., Bartos, I., Omukai, K., *et al.*: Mass-gap Mergers in Active Galactic Nuclei. The Astrophysical Journal **908**, 194 (2021) https://doi.org/10.3847/1538-4357/abd555

[5] Ford, K.E.S., McKernan, B.: Binary black hole merger rates in AGN discs versus nuclear star clusters: Loud beats quiet. Monthly Notices of the Royal Astronomical Society **517**, 5827–5834 (2022) https://doi.org/10.1093/mnras/stac2861

[6] Graham, M.J., Ford, K.E.S., McKernan, B., Ross, N.P., Stern, D., *et al.*, : Candidate Electromagnetic Counterpart to the Binary Black Hole Merger Gravitational-Wave Event S190521g*. Physical Review Letters **124**, 251102 (2020) https://doi.org/10.1103/PhysRevLett.124.251102

[7] Popa, S.A., de Mink, S.E.: Very Massive, Rapidly Spinning Binary Black Hole Progenitors through Chemically Homogeneous Evolution—The Case of GW231123. The Astrophysical Journal **995**, 76 (2025) https://doi.org/10.3847/

2041-8213/ae20f1

[8] Li, Y.-J., Tang, S.-P., Xue, L.-Q., Fan, Y.-Z.: GW231123: Likely a Product of Successive Mergers from ∼10 Stellar-mass Black Holes. The Astrophysical Journal **999**, 127 (2026) https://doi.org/10.3847/1538-4357/ae4102

[9] Delfavero, V., Ray, S., Cook, H.E., Nathaniel, K., McKernan, B., *et al.*, : Prospects for the Formation of GW231123 from the AGN Channel. arXiv (2025). https://doi.org/10.48550/arXiv.2508.13412

[10] Kimball, C., Talbot, C., Berry, C.P.L., Carney, M., Zevin, M., *et al.*, : Black Hole Genealogy: Identifying Hierarchical Mergers with Gravitational Waves. The Astrophysical Journal **900**, 177 (2020) https://doi.org/10.3847/1538-4357/aba518

[11] Stegmann, J., Olejak, A., de Mink, S.E.: Resolving Black Hole Family Issues among the Massive Ancestors of Very High-spin Gravitational-wave Events like GW231123. The Astrophysical Journal **992**, 26 (2025) https://doi.org/10.3847/2041-8213/ae0e5f

[12] Plunkett, C., Callister, T., Zevin, M., Vitale, S.: Signatures of a Subpopulation of Hierarchical Mergers in the GWTC-4 Gravitational-Wave Dataset. arXiv (2026). https://doi.org/10.48550/arXiv.2601.07908

[13] Tong, H., Callister, T.A., Fishbach, M., Thrane, E., Antonini, F., *et al.*, : A Subpopulation of Low-Mass, Spinning Black Holes: Signatures of Dynamical Assembly. arXiv (2025). https://doi.org/10.48550/arXiv.2511.05316

[14] Kimball, C., Talbot, C., Berry, C.P.L., Zevin, M., Thrane, E., *et al.*, : Evidence for Hierarchical Black Hole Mergers in the Second LIGO-Virgo Gravitational Wave Catalog. The Astrophysical Journal **915**, 35 (2021) https://doi.org/10.3847/2041-8213/ac0aef

[15] Abac, A.G., Abouelfettouh, I., Acernese, F., Ackley, K., Adamcewicz, C., *et al.*, : GW241011 and GW241110: Exploring Binary Formation and Fundamental Physics with Asymmetric, High-spin Black Hole Coalescences. The Astrophysical Journal **993**, 21 (2025) https://doi.org/10.3847/2041-8213/ae0d54

[16] LIGO Scientific Collaboration, Virgo Collaboration, KAGRA Collaboration: GW241011 and GW241110: Exploring Binary Formation and Fundamental Physics with Asymmetric, High-spin Black Hole Coalescences. Zenodo (2025). https://doi.org/10.5281/zenodo.17343574

[17] Pretorius, F.: Evolution of Binary Black-Hole Spacetimes. Physical Review Letters **95**, 121101 (2005) https://doi.org/10.1103/PhysRevLett.95.121101

[18] Buonanno, A., Kidder, L.E., Lehner, L.: Estimating the final spin of a binary

black hole coalescence. Physical Review D **77**, 026004 (2008) https://doi.org/10.1103/PhysRevD.77.026004

[19] Biscoveanu, S., Callister, T.A., Haster, C.-J., Ng, K.K.Y., Vitale, S., *et al.*: The Binary Black Hole Spin Distribution Likely Broadens with Redshift. The Astrophysical Journal **932**, 19 (2022) https://doi.org/10.3847/2041-8213/ac71a8

[20] Farah, A.M., Vijaykumar, A., Fishbach, M.: The Steep Redshift Evolution of the Hierarchical Binary Black Hole Merger Rate May Cause the z-χeff Correlation. The Astrophysical Journal **1001**, 40 (2026) https://doi.org/10.3847/2041-8213/ae4e19

[21] Adamcewicz, C., Thrane, E.: Do unequal-mass binary black hole systems have larger χeff? Probing correlations with copulas in gravitational-wave astronomy. Monthly Notices of the Royal Astronomical Society **517**, 3928–3937 (2022) https://doi.org/10.1093/mnras/stac2961

[22] Adamcewicz, C., Lasky, P.D., Thrane, E.: Evidence for a Correlation between Binary Black Hole Mass Ratio and Black Hole Spins. The Astrophysical Journal **958**, 13 (2023) https://doi.org/10.3847/1538-4357/acf763

[23] Vijaykumar, A., Farah, A.M., Fishbach, M.: The Maximum Mass Ratio of Hierarchical Binary Black Hole Mergers May Cause the q-χeff Correlation. The Astrophysical Journal **999**, 30 (2026) https://doi.org/10.3847/2041-8213/ae4878

[24] The LIGO Scientific Collaboration, the Virgo Collaboration, the KAGRA Collaboration, Abac, A.G., Abouelfettouh, I., *et al.*, : GWTC-4.0: Population Properties of Merging Compact Binaries. arXiv (2025). https://doi.org/10.48550/arXiv.2508.18083